Journal of Power Sources 196 (2011) 4226–4235

Contents lists available at ScienceDirect

Journal of Power Sources

journal homepage: www.elsevier.com/locate/jpowsour

Pt and PtRu electrocatalysts supported on carbon xerogels for direct methanol fuel cells

C. Alegre[a], L. Calvillo[a], R. Moliner[a], J.A. González-Expósito[b], O. Guillén-Villafuerte[b], M.V. Martínez Huerta[c], E. Pastor[b], M.J. Lázaro[a,*]

[a] Instituto de Carboquímica (CSIC), Miguel Luesma Castán 4, 50018 Zaragoza, Spain
[b] Universidad de La Laguna, Dpto de Química-Física, Avda. Astrofísico Francisco Sánchez s/n, 38071 La Laguna (Tenerife), Spain
[c] Instituto de Catálisis y Petroleoquímica (CSIC), C/Marie Curie, 2, 28049 Madrid, Spain

ARTICLE INFO

Article history:
Received 20 July 2010
Received in revised form
23 September 2010
Accepted 18 October 2010
Available online 26 October 2010

Keywords:
Pt
PtRu
DMFC
Carbon xerogel
Functionalization
CO and methanol oxidation

ABSTRACT

Carbon xerogels (CXs) have been prepared by polycondensation of resorcinol and formaldehyde in water by the sol–gel method. Functionalization with diluted and concentrated nitric acid as oxidizing agents was carried out to create surface oxygen groups, acting as anchoring sites for metallic particles. Characterization techniques included nitrogen physisorption, scanning electron microscopy, temperature programmed desorption and temperature programmed oxidation. Functionalized xerogels were used as supports to synthesize Pt and PtRu electrocatalysts by a conventional impregnation method. Catalysts electrochemical activity towards the oxidation of methanol was studied by cyclic voltammetry and chronoamperometry to establish the effect of the surface chemistry on the catalysts synthesis. Carbon monoxide oxidation was also studied to determine the electrochemical active area and the CO tolerance of the as prepared catalysts. Results were compared to those obtained with commercial Pt/C and PtRu/C catalysts supported on Vulcan XC-72R (E-TEK). All electrocatalysts supported on carbon xerogel showed better performances than commercial ones, providing higher current density values for the oxidation of methanol.

© 2010 Elsevier B.V. All rights reserved.

1. Introduction

Direct methanol fuel cells (DMFCs) are regarded as promising power sources for portable electronic devices and domestic and automotive applications, having the advantages of ease of handling of the fuel and flexibility of cell operation [1]. However the commercialization of DMFCs is still hindered by some technical challenges, mainly: (1) slow kinetics of methanol oxidation reactions at the anode at low temperatures and (2) methanol crossover [2]. Pt-based catalysts have been widely recognized as the best electrocatalysts for DMFCs. However, the limited availability and high price of Pt are significant barriers to the widespread use of this type of fuel cells. To reduce the cost of fuel cells, one of the important challenges is the development of Pt free catalysts or catalysts with a lower content of this metal. For this reason, binary and ternary Pt-based catalysts and non-Pt-based ones have been tested as electrode materials for DMFCs [3]. Among bimetallic Pt catalysts, the Pt–Ru system is the best known for its activity in the electrochemical methanol oxidation reaction [4–8]. At room temperature methanol does not oxidize on Ru but this metal can promote the oxidation of CO adsorbed as intermediate of this reaction on Pt at more negative potentials [9]. The formation of an oxygenated species on Pt is reputedly difficult, as Pt–OH groups are only formed, in substantial quantities, above ca. +0.7 V vs. RHE. Ru is more easily oxidized than Pt and thus is able to oxidize the methanol adsorbate at a lower potential. The promotor acts via a so-called bi-functional mechanism, as was suggested for Ru [10]. Nevertheless the efficiency of the DMFC operating with this catalyst is still insufficient for practical applications. Therefore, further optimization of the anode material for DMFC is necessary for its development and commercialisation.

In this context, an attractive approach that appears as a possible solution to reduce Pt loading and increase the catalytic efficiency is to use novel carbonaceous materials as support. The nature of the support as well as the interaction between the former and the metal have been demonstrated to be extremely important, given that determines the physicochemical properties of catalysts, such as dispersion, stability and morphology of metallic crystallites [11–13]. In addition, characteristics of the support can also determine the electrochemical properties of catalysts by altering mass transport, active electrochemical area and metal nanoparticle stability during the cell operation [14,15]. Hence, the optimization of carbon supports is very important in DMFC technology development.

* Corresponding author. Tel.: +34 976 733977; fax: +34 976 733318.
E-mail address: mlazaro@icb.csic.es (M.J. Lázaro).

0378-7753/$ – see front matter © 2010 Elsevier B.V. All rights reserved.
doi:10.1016/j.jpowsour.2010.10.049

Among all kinds of carbon supports, carbon blacks are the most commonly materials used as support in the preparation of commercial electrocatalysts for DMFCs, being Vulcan XC-72R the most widely used support. This material shows high mesoporous distribution and high electrical conductivity [16]. However, although Vulcan XC-72R has a suitable specific surface area, it still exhibits insufficient properties for this purpose. This is due to other factors, such as pore size distribution or surface chemistry, that also affect the preparation and performance of the electrocatalysts. For this reason, novel non-conventional carbon materials are being studied as electrocatalyst support in order to replace Vulcan XC-72R. Among these novel carbon material, carbon nanotubes [2,11], carbon nanofibers [17–20] ordered mesoporous carbons [21] and carbon xerogels and aerogels [1,11,19,22–30] are being studied.

Carbon xerogels are attracting much attention for their unique and controllable properties, such as high surface area, mesopore structure with narrow pore size distribution, and high purity, which in turn, are attributed to the synthesis reaction mechanism, being similar to the sol–gel process. Their preparation, consisting on the polycondensation of resorcinol with formaldehyde followed by drying and pyrolysis, avoids supercritical drying required for the synthesis of carbon aerogels, offering great advantages in terms of cost and safety [1]. Besides, their three-dimensionally interconnected uniform pore structure allows a high degree of dispersion of the active phase and an efficient diffusion of reagents.

Some papers have appeared in the literature during the last decade concerning the use of carbon aerogels and xerogels as catalysts supports. Rolison and co-workers synthesized highly active electrocatalytic nanostructured architectures constructed from colloidal-Pt-modified carbon–silica composite aerogels. These materials increased by 4 orders of magnitude per gram of Pt the electrocatalytic activity for methanol oxidation than Pt-modified carbon powder [31]. More recently, the same group prepared thiophene-modified aerogels. The sulphur-functionalized carbon aerogel was tested in CO-stripping voltammetry and examined for oxygen reduction activity, in order to study the ability of the material to mimic the thiophene-mediated precious metal binding occurring with Vulcan carbon. The results obtained suggested that these functionalized nanoarchitectures may improve the applicability of carbon aerogel electrode structures for fuel cell and other electrocatalytic applications [32].

Job and co-workers [22] prepared Pt/C catalysts by impregnation using three xerogels with various pore textures as supports. The specific catalytic activity obtained for benzene hydrogenation was 4–10 times higher than that obtained with active charcoal-supported catalysts prepared by a similar method. The high dispersion of Pt was attributed to the presence in the xerogel of large mesopore or macropore volumes, which facilitates impregnation.

In a more recent paper [33], the same group synthesized carbon xerogels with various pore textures by evaporative drying and pyrolysis of resorcinol–formaldehyde gels, and used them as supports for Pt catalysts in PEM fuel cell cathodes. Results were compared with those for catalysts supported on carbon aerogels, yielding similar performances.

On the other hand, Mastragostino and co-workers [3] studied the specific catalytic activity of DMFC anodes based on PtRu catalysts deposited by chemical and electrochemical route on mesoporous cryo- and xerogel carbons. Their results were compared with those obtained with PtRu supported on Vulcan, being the specific catalytic activity more than double when Vulcan is substituted by former carbons.

Finally, Samant and co-workers [23] also synthesized highly mesoporous carbon via sol–gel condensation of resorcinol and formaldehyde. Electrooxidation of methanol in alkaline electrolyte was carried out using Pt and PtNi catalysts supported on highly mesoporous carbon xerogels. The electrocatalytic tests showed better performance of the catalysts when impregnated on this kind of carbon support.

In a more recent work [13], the same group prepared multiwalled carbon nanotubes and high surface area mesoporous carbon xerogel and used them as supports for monometallic Pt and bimetallic PtRu catalysts. In order to assess the influence of the oxygen surface groups of the support, the mesoporous carbon xerogel was also oxidized with diluted oxygen before impregnation. A remarkable increase in the activity was observed when the PtRu catalysts were supported on the oxidized xerogel. This effect was explained in terms of the metal oxidation state. It was shown that the oxidized support helps to maintain the metals in the metallic state, as required for the electro-oxidation of methanol.

In this paper, mesoporous carbon xerogels have been synthesized and functionalized by different oxidation treatments. Then, Pt and PtRu nanoparticles have been deposited by an impregnation method on the as-prepared xerogels. Physicochemical properties of catalysts have been studied by X-ray (EDX, XRD) and microscopic (TEM) methods in order to determine the influence of the support. On the other hand, cyclic voltammetry and chronoamperometry have been used to analyze the influence of the support on the activity towards carbon monoxide and methanol oxidation. Commercial Pt and PtRu supported catalysts (E-TEK) have also been studied for comparison.

2. Experimental

2.1. Synthesis of carbon xerogels

Resorcinol(1,3-dihydroxybenzoic acid)–formaldehyde organic gels were synthesized by the sol–gel method first proposed by Pekala [25]. The necessary amounts of resorcinol (*R*) (98% Sigma–Aldrich) and sodium carbonate deca-hydrated (*C*) (Panreac) (molar ratio $R/C = 50$) were dissolved in 120 mL of deionized water under stirring. Subsequently, the required volume of formaldehyde (*F*) (37 wt.% aqueous solution, Sigma–Aldrich) (molar ratio $R/F = 0.5$) was added to the former mixture and pH was adjusted to 6 with an aqueous solution of 2 M HNO_3. The mixture was stirred for 30 minutes and then poured into sealed flasks, followed by curing for 24 h at room temperature, 24 h at 50 °C and 5 days at 85 °C until curing was complete as described elsewhere [26]. Afterwards gels were washed with acetone for three days to exchange the initial solvent, water. Acetone was daily replaced after vacuum filtration. This procedure allows keeping the original gel structure, as surface tension caused by evaporation of the solvent is lower for acetone than for water [30]. Finally, wet gels were dried in an oven at 65 °C and held for 5 h, and then, temperature was risen up to 110 °C and held for another 5 h, as described elsewhere [27]. Pyrolysis of all organic gels was carried out in a tubular furnace at 800 °C for 3 h under a flow of 100 mL min^{-1} N_2.

2.2. Carbon xerogel functionalization

Carbon xerogels were oxidized under different conditions in order to create surface oxygen groups that act as anchoring sites for metallic particles, besides improving its dispersion onto the support [34–38]. The oxidation treatments were performed at room temperature with 2 M and concentrated HNO_3 (65%) for 30 and 120 min. Oxidized materials were subsequently washed with deionized water until complete removal of the acid, and dried in an oven at 108 °C for 24 h. Carbon xerogels so obtained were named as follows: for example, CX_Nc_30 corresponds to a carbon xerogel (CX) where Nc (or Nd) stands for concentrated (or diluted) nitric acid, and numbers (30 or 120) correspond to the duration (min) of the oxidation process.

2.3. Pt and PtRu catalysts synthesis

Pt and PtRu were deposited on former functionalized carbon xerogels by impregnation and reduction with sodium borohydride [39]. The amount of metallic precursors was calculated to obtain a metal loading of 20% w/w. In the case of PtRu catalysts the nominal atomic ratio Pt:Ru was 1:1. An aqueous solution of H_2PtCl_6 (Sigma–Aldrich) (for Pt/CX catalysts) or H_2PtCl_6 and $RuCl_3$ (Sigma–Aldrich) (for PtRu/CX catalysts), was slowly added to a dispersion of carbon xerogel in ultrapure water under sonication. pH was adjusted to 5 with a NaOH solution. Metals were reduced by addition of sodium borohydride, maintaining temperature around 18 °C. Subsequently, catalysts were filtered and thoroughly washed with ultrapure water, and dried overnight at 60 °C.

2.4. Carbon xerogels and catalysts textural, structural and morphological characterization

The nature and characteristics of carbon xerogels were determined using nitrogen physisorption, temperature programmed desorption (TPD), temperature programmed oxidation (TPO) and scanning electron microscopy (SEM).

Textural properties such as specific surface area, pore volume and mesoporosity were calculated from nitrogen adsorption–desorption isotherms, measured at −196 °C using a Micromeritics ASAP 2020. Total surface area and pore volume were determined using the Brunauer–Emmet–Teller (BET) equation and the single point method, respectively. Microporosity was determined from *t*-plot method, and mesoporosity as the difference between the total pore and micropore volume.

Surface chemistry of carbon supports was studied by TPD experiments. Such experiments were performed in a Micromeritics Pulse Chemisorb 2700 equipment, under a flow of helium with a heating rate of 10 °C min^{-1} from 150 °C up to 1050 °C. The amounts of CO and CO_2 desorbed from the samples were analyzed by gas chromatography in a HP 5890 chromatograph with a thermal conductivity detector, packed columns Porapak N 10 ft and molecular sieve. These experiments give information about the surface oxygen groups created during the oxidation treatments. Acidic groups (carboxylic groups, lactones and anhydrides) are decomposed into CO_2 at low temperatures and basic and neutral groups (anhydrides, phenols and quinones) are decomposed into CO at high temperatures [35].

Stability under oxidation conditions was studied by means of TPO. These experiments were carried out under a flow of air using a heating rate of 5 °C min^{-1} from room temperature up to 800 °C on a Setaram Setsys Evolution thermogravimetric analyzer.

Finally, the morphology of carbon xerogels was studied by SEM, using a Hitachi S-3400 N microscope. SEM combined with Energy Dispersive X-Ray Spectroscopy (SEM-EDX) was used to determine the amount of metal deposited. An analyzer EDX Röntec XFlash of Si(Li) was employed with this purpose.

The electrical resistance that a powdered material offers to electrical current is a combination of the individual resistances of both the grains and the contacts between them. Consequently, measuring the conductivity of a powder requires pressing on the bed of grains in order to ensure the electrical contact [46]. The device used with this purpose consists on a thick-walled PVC tube with an inner diameter of 8 mm. A scheme of the experimental set-up and the equivalent electrical circuit are shown in Fig. 1(a) and (b) respectively. The bottom of the cylinder is closed by a stationary brass piston and, after introducing 2 cm^3 of weighted sample, the upper side is closed by a stainless steel plunger, allowed to move down in the cylinder. Then several weighted loads are put on the upper piston and the pressure reaches values from 0.6 MPa to 9.32 MPa, which are high enough to allow good electrical contacts between grains, but too low to cause the crushing of the particles. The height of the sample is measured by using a micrometer Mitutoyo. Then the dc electrical resistance of the pressed powder is determined by a two-probe method. The sample and a calibrated resistor are connected acting as resistors in series, as it is schematized in Fig. 1. Known values of voltage are then applied by a power supply Array 3645A, scanning current values up to 20 mA, and voltage drop in the two resistors are measured with a 6½ digits Array M3500A multimeter. Electrical conductivity is then calculated from resistance value, obtained in turn from the adjustment of voltage and current slope, and geometric parameters.

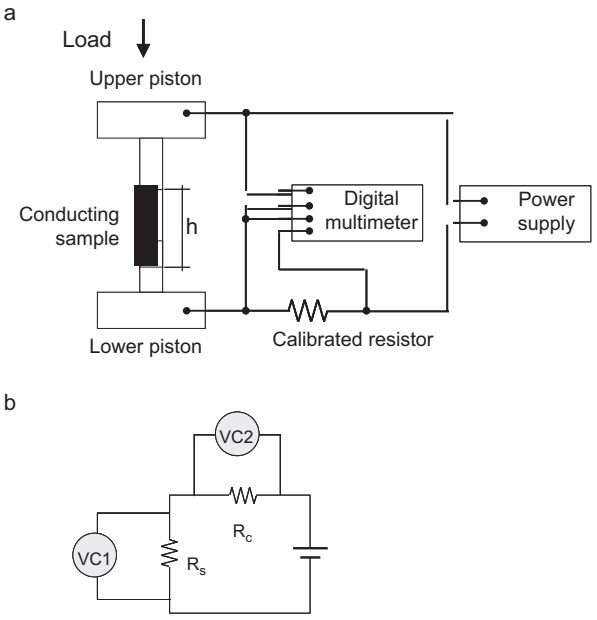

Fig. 1. (a) Scheme of the experimental devices for the measurement of electrical conductivity of carbonaceous powders. (b) Equivalent electrical circuit of the device.

Catalysts were characterized by X-ray diffraction (XRD), using a Bruker AXS D8 Advance diffractometer, with a θ–θ configuration and using Cu-Kα radiation.

Particle sizes were evaluated from TEM images obtained in a JEOL 2100F microscope operated with an accelerating voltage of 200 kV and equipped with a field emission electron gun providing a point resolution of 0.19 nm. The standard procedure involved dispersing 3 mg of the sample in ethanol in an ultrasonic bath for 15 min. The sample was then placed in a Cu carbon grid where the liquid phase was evaporated.

2.5. Electrochemical characterization

Catalysts electrochemical activity towards the oxidation of carbon monoxide and methanol was studied by cyclic voltammetry and chronoamperometry. A flow cell with a three-electrode assembly at room temperature and an AUTOLAB potentiostat–galvanostat

Table 1
Carbon xerogels textural properties.

Sample	Surface area ($m^2\ g^{-1}$)	Total volume ($cm^3\ g^{-1}$)	Mesopore volume ($cm^3\ g^{-1}$)	% Mesopores in terms of pore volume
CX	577	1.83	1.65	90.6
CX_Nd_30	576	1.81	1.63	90.4
CX_Nd_120	566	1.73	1.56	90.9
CX_Nc_30	524	1.67	1.52	90.6
CX_Nc_120	519	1.67	1.51	90.7
Vulcan XC-72R	224	0.47	0.46	98.2

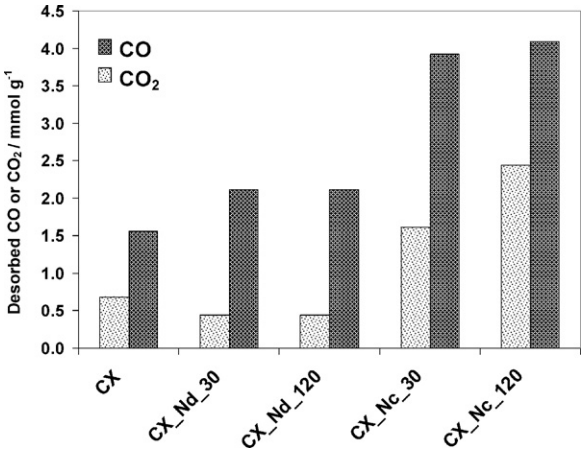

Fig. 2. mmol g^{-1} of surface oxygen groups desorbed as CO or CO_2 in TPD experiments.

were used to carry out the electrochemical characterization. The counter electrode consisted on a pyrolitic graphite rod and the reference electrode was a reversible hydrogen electrode (RHE). All potentials in the text are referred to the latter. The working electrode consisted of a pyrolitic graphite disk with a thin layer of the different electrocatalysts deposited onto it. For the preparation of this layer, an aqueous suspension of Pt/CX or PtRu/CX catalysts was obtained by ultrasonically dispersing it in Nafion and ultrapure water (Millipore). Subsequently an aliquot of 40 μL of the dispersed suspension was deposited on top of the graphite disk (7 mm) and dried under inert atmosphere prior its use. After preparation, the electrode was immersed into deaerated 0.5 M H_2SO_4 electrolyte, prepared from high purity reagents (Merck) and ultrapure water (Milli-Q). The electrolyte was saturated with pure N_2 or CO (99.997%, Air Liquide), depending on the experiments.

Activation of the electrode was performed by potential cycling solution between 0.05 and 1.10 V (for Pt/CX catalysts) or 0.85 V vs. RHE (for PtRu/CX catalysts) at a scan rate of 0.5 V s^{-1} until a stable voltammogram in the base electrolyte (0.5 M H_2SO_4) was obtained. The upper limit for potential cycling was established at 0.85 V for PtRu materials to avoid partial dissolution of Ru from the alloy.

CO stripping voltammograms were obtained after bubbling this gas in the cell for 10 min at 0.20 V, followed by electrolyte exchange and nitrogen purging to remove the excess of CO, and oxidation by scanning the potential up to the upper limit previously established for Pt and PtRu catalysts. The admission potential was selected

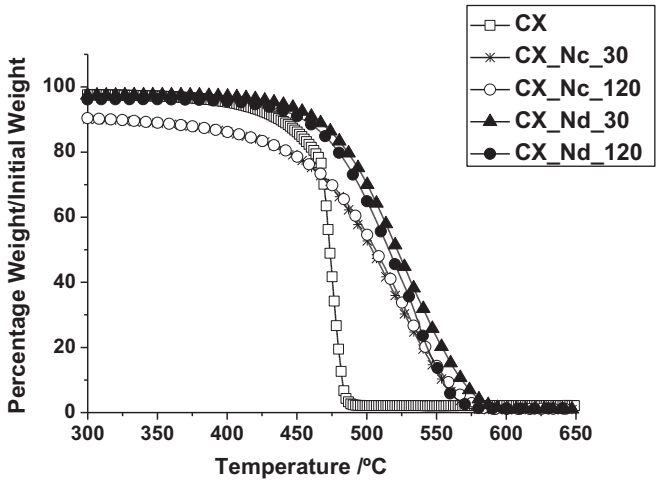

Fig. 3. TPO profiles of untreated and functionalized carbon xerogels.

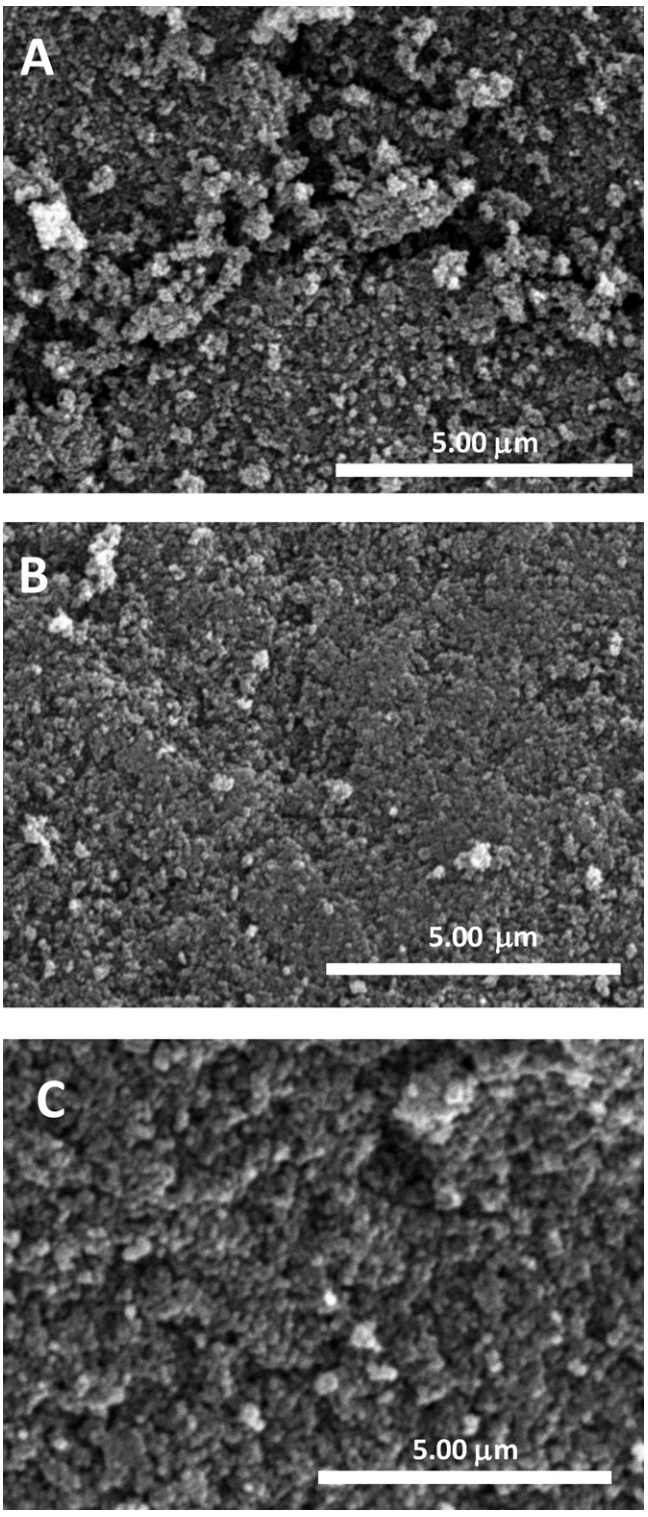

Fig. 4. SEM micrographs of carbon xerogels: (A) CX_unoxidized; (B) CX_Nd_120 and (C) CX_Nc_120.

considering that, for this value, maximum adsorbate coverage is achieved for CO adsorption on Pt and PtRu. Electrochemical Pt and PtRu active areas were determined from the integration of the current involved in the oxidation of a CO monolayer taking into account that CO adsorbs on both Pt and Ru and assuming 420 μC cm^{-2}. Current was normalized with respect to this electroactive area.

Cyclic voltammograms for the electrooxidation of methanol were carried out in a 2 M CH_3OH + 0.5 M H_2SO_4 solution, at scan

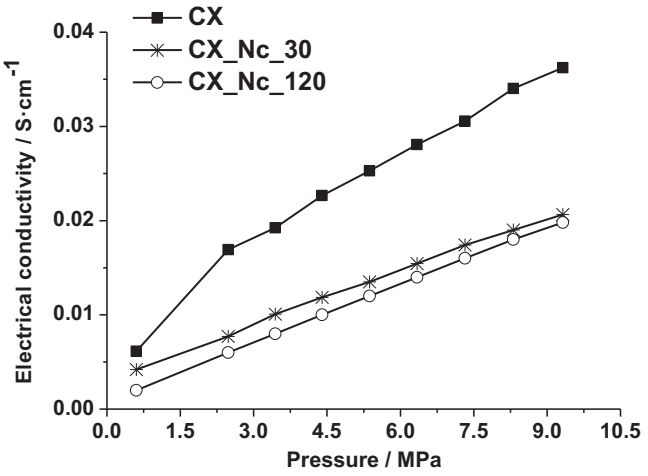

Fig. 5. Apparent electrical conductivity of CXs vs. applied pressure.

Table 2
Pt electrocatalysts properties.

Sample	% w/w Pt	Pt crystal size (nm)
Pt/CX	8.7	5.0
Pt/CX_Nd_30	13.3	3.2
Pt/CX_Nd_120	14.2	5.0
Pt/CX_Nc_30	10.0	4.4
Pt/CX_Nc_120	10.1	3.5

rate of 0.02 V s^{-1}, between 0.0 and 1.10 for Pt/CX or between 0.0 and 0.85 V for PtRu/CX.

Chronoamperometries were performed at 0.60 V in a 2 M CH_3OH + 0.5 M H_2SO_4 solution in order to evaluate the performance of the electrocatalysts for the oxidation of methanol. Every experiment was carried out at room temperature (25 ± 1 °C), and current was normalized with respect to the electroactive area.

3. Results and discussion

3.1. Carbon xerogels properties and functionalization

Textural properties of functionalized xerogels determined from nitrogen physisorption isotherms are shown in Table 1. High surface area values (between 518 and 577 m^2 g^{-1}) as well as mesopore volumes (between 1.51 and 1.65 cm^3 g^{-1}; ca. 90% total volume) are obtained. These textural properties make carbon xerogels appropriate supports for an optimum metal deposition [20,27,30]. As can be seen in the table, functionalization with diluted nitric acid (lighter conditions) barely affect textural properties, while more severe conditions (concentrated nitric acid) lead to a slight reduction of surface area and volume, but CXs still maintain a high mesoporosity. By comparison with the commercial support, Vulcan XC-72 (223 m^2 g^{-1} and 0.47 cm^3 g^{-1}), carbon xerogels present higher surface area and pore volume.

Table 3
PtRu electrocatalysts properties.

Sample	% Total metal	% w/w Pt	% w/w Ru	Atomic ratio Pt:Ru	PtRu crystal size (nm)
PtRu/CX	12.8	8.8	4.0	53: 47	3.5
PtRu/CX_Nd_30	17.2	12.1	5.1	55: 45	2.5
PtRu/CX_Nd_120	14.9	8.3	6.6	40: 60	3.7
PtRu/CX_Nc_30	15.9	10.5	5.4	45: 55	nd
PtRu/CX_Nc_120	16.4	10.8	5.6	50: 50	4.9

nd, Particle size below detection limits (2 nm).

Surface chemistry of carbon xerogels was studied by means of TPD. These experiments give information about the surface oxygen groups created during the oxidation treatments. CO and CO_2 profiles were deconvoluted to determine the nature and the amount of the desorbed groups but, according to previous publications [35,40], some assumptions were needed. Thus, CO_2 evolution is considered as the addition of three contributions corresponding to carboxylic acids, anhydrides and lactones. However, one mol of an anhydride group decomposes releasing one mol of CO and one mol of CO_2, and therefore, anhydrides contribute to both signals. Apart from anhydrides, the CO curve decomposes into phenols and carbonyl/quinones. In the case of functionalized carbon xerogels, the major contribution comes from groups desorbed as CO [35]. It was observed that the more severe the treatment, the higher the amount of surface oxygen groups created [17,41,42]. Fig. 2 shows that treatments with diluted HNO_3 barely increase the amount of oxygen groups, while treatments with concentrated HNO_3 increase the amount of them.

The resistance of the carbon support towards oxidation in air was studied with TPO experiments. As can be seen in Fig. 3, carbon xerogels begin to oxidize around 420 °C. It can also be observed that functionalization treatments slightly increase carbon xerogels resistance towards oxidation. The morphology of carbon xerogels was studied by SEM, obtaining small polymer particles (3–5 nm) that are interconnected with large necks (giving the gel a fibrous appearance), what is the morphology expected for xerogels synthesized with a low R/C ratio [28] (Fig. 4). From the micrographs it can be concluded that functionalization treatment does not seem to have any influence on the morphology of the carbon materials.

Fig. 5 shows some examples of the electrical conductivity of carbon xerogels (unoxidized and oxidized with concentrated nitric acid) depending on the applied pressure (from 0.6 MPa to 9.32 MPa values). It has been reported in literature that increasing pressure implies an increase in the number of contacts between the grains and consequently electrical resistance diminishes [46,47]. What can be observed in the figure is that the electrical conductivity of

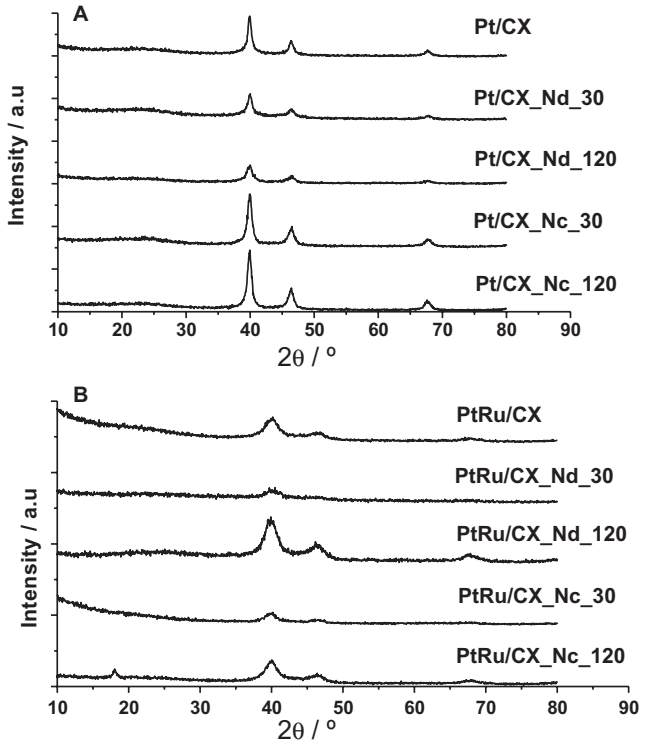

Fig. 6. Diffractograms obtained by XRD for (A) Pt/CX catalysts. (B) PtRu/CX catalysts.

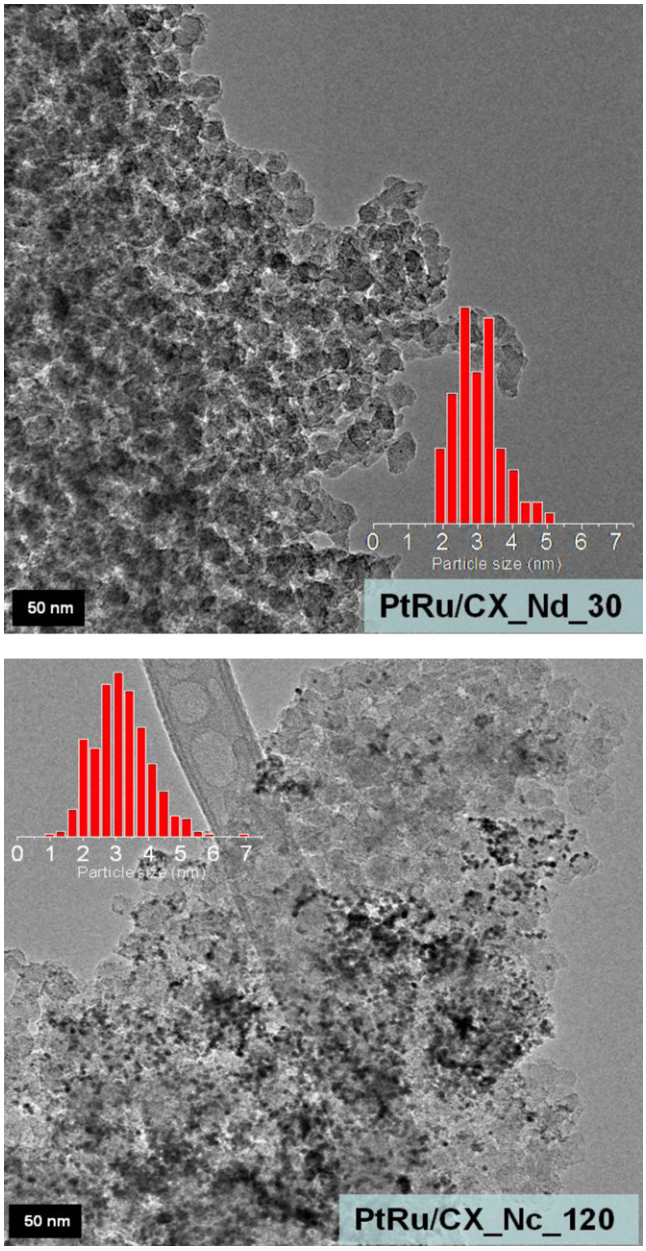

Fig. 7. TEM micrographs for the electrocatalysts: PtRu/CX_Nd_30 and PtRu/CX_Nc_120. The inset shows the Pt/Ru particle size distribution in the electrocatalysts.

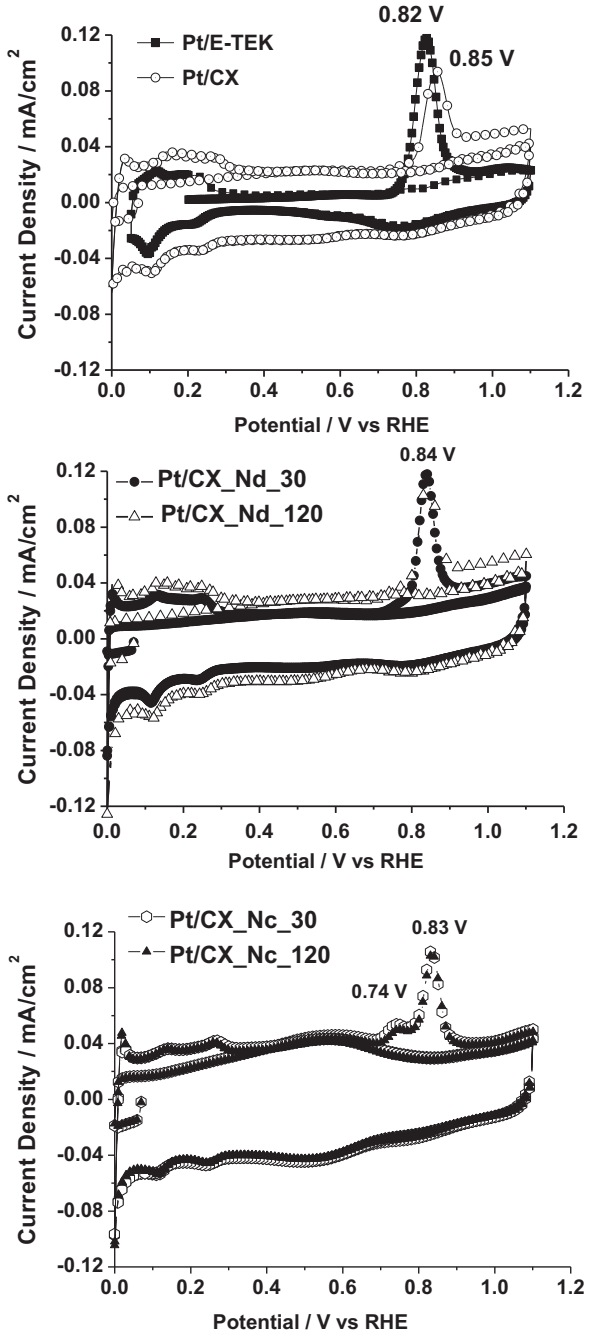

Fig. 8. Cyclic voltammograms during CO stripping for Pt/CX catalysts and Pt/E-TEK in a 0.5 M H_2SO_4 solution. Scan rate $\nu = 0.02\ V\ s^{-1}$.

the powder increases with pressure and that after functionalization treatments, the electrical conductivity decreases. The high amount of surface oxygen groups is responsible for the worse electrical contact between particles, what leads to a decrease in the electrical conductivity [48].

3.2. CXs-supported Pt and PtRu catalysts

Pt and PtRu catalysts supported on functionalized carbon xerogels were characterized by SEM-EDX and XRD. Their properties are summarized in Tables 2 and 3. SEM-EDX analyses were carried out to determine the percentage of metal deposited and the composition of the alloy in the case of PtRu materials. As shown in Table 3, the atomic ratio Pt:Ru is similar for all materials (1:1).

In the case of Pt catalysts, functionalized supports seem to better anchor metallic particles obtaining higher metal content, probably due to the higher amount of carbonyl and quinones surface oxygenated groups (carbon surface basic sites) which have been established to be responsible for the strong adsorption of Pt on carbon [36]. For PtRu materials, similar effect is observed although less pronounced than for Pt/C.

Pt and PtRu crystallite sizes (Tables 2 and 3) were obtained from the 220 peak in the XRD diffractograms shown in Fig. 6 using the Scherrer's equation. Values range from 3.5 to 5.0 nm, with the exception of PtRu/CX_Nc_30 where the calculation cannot be made, probably due to a small size below the detection limit of the technique (2 nm). From these data it can be concluded that crystallite sizes are not directly related with the number of oxygenated groups on the surface, i.e. with the functionalization process.

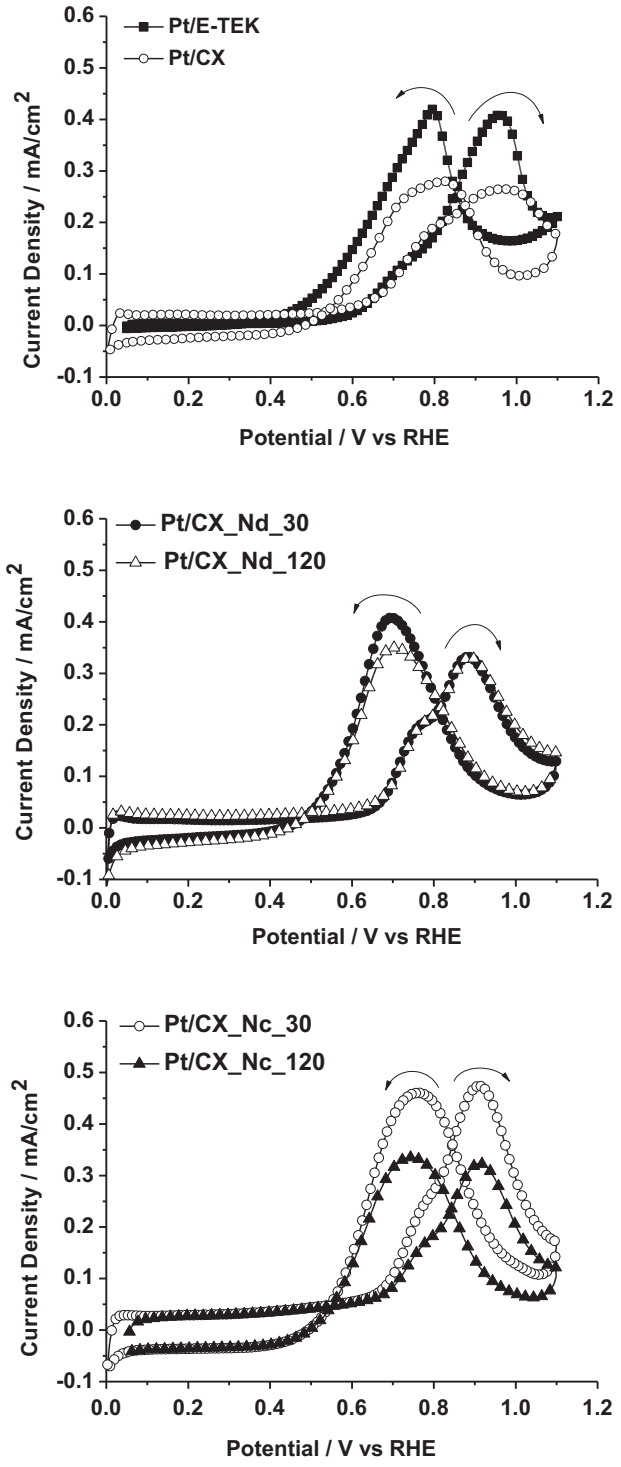

Fig. 9. Cyclic voltammograms for the electrooxidation of methanol in a 2 M CH_3OH + 0.5 M H_2SO_4 solution at Pt/CX catalysts and Pt/E-TEK. Scan rate $\nu = 0.02\ V\ s^{-1}$.

This assumption has been corroborated applying TEM (Fig. 7): smaller PtRu particles with a narrower size distribution are obtained for materials prepared with CX_Nd_30 support in comparison with CX_Nc_120. It is also observed that catalysts supported on xerogels with a stronger functionalization treatment (CX_Nc_120) and a high metallic content, show metal agglomerates; whereas catalysts supported on xerogels with a less severe functionalization treatment (CX_Nd_30), presented high and homogeneous metallic dispersion as can be seen in the micrographs.

3.3. Electrochemical studies

3.3.1. Pt catalysts supported on functionalized carbon xerogels

Pt catalysts supported on functionalized carbon xerogels were characterized by cyclic voltammetry and CO stripping was performed in order to establish the influence of the support and its functionalization on the potential for its oxidation. Fig. 8 shows the CO-stripping voltammograms obtained for Pt based catalysts. The second cycles recorded after CO-stripping, which correspond to the voltammograms in the base electrolyte for clean surfaces, are also shown. The CO_{ad} oxidation peak potential on Pt (E-TEK) was obtained around 0.82 V, as reported in the literature for commercial catalysts. In the case of Pt/CX, Pt/CX_Nd_30 and Pt/CX_Nd_120 catalysts, this contribution is centred at 0.84 V; however, for these catalysts the onset for electrooxidation of CO occurred at more negative potentials with respect to the commercial catalyst.

For Pt catalysts supported on carbon xerogels oxidized with concentrated HNO_3, two oxidation peaks (not observed for the other catalysts) can be observed: one at high potentials (around 0.83 V) and another one at more negative potentials, around 0.74 V. This second peak could be related with the presence of oxygen groups at the support, which contribute to the oxidation of CO in someway. Accordingly, xerogels-supported platinum catalysts are expected to be less poisoned with CO when used in a polymer electrolyte fuel cell.

It is remarkable in the CVs the differences in the current densities observed in the double layer region (0.4–0.6 V) for the catalysts supported on Vulcan XC-72R (E-TEK) and on the xerogels. At 0.4 V, the double layer current density (from the second voltammetric scan) is about 4 times higher for the untreated CX and those treated with diluted nitric acid, and about 7 times higher for the CX treated with the concentrated acid. This implies that the capacitive behaviour is more apparent for catalysts supported on CX with respect to Vulcan XC-72R and can be increased with the severity of the oxidation treatment.

The behaviour of the electrocatalysts towards the oxidation of methanol was studied in a deaerated 2 M CH_3OH + 0.5 M H_2SO_4 solution. Resulting cyclic voltammograms are given in Fig. 9. As can be observed, the onset potential of methanol electrooxidation for catalysts supported on carbon xerogels occurs at similar potentials (around 0.6 V) than for the commercial one. The current densities are quite similar for all materials, but slightly higher values are observed at the oxidation peaks for Pt/CX_Nc_30 catalyst. As previously commented for CO oxidation, the electronic interaction between metallic particles and carbon support,

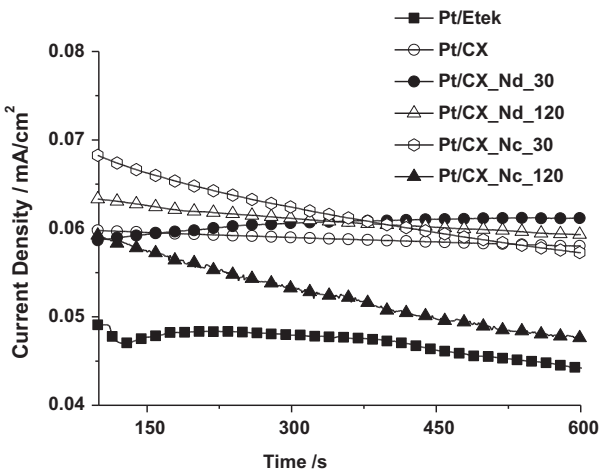

Fig. 10. Current density–time curves recorded in a 2 M H_2SO_4 + 0.5 M CH_3OH solution at E = 0.60 V vs. RHE for Pt/CX catalysts and Pt/E-TEK.

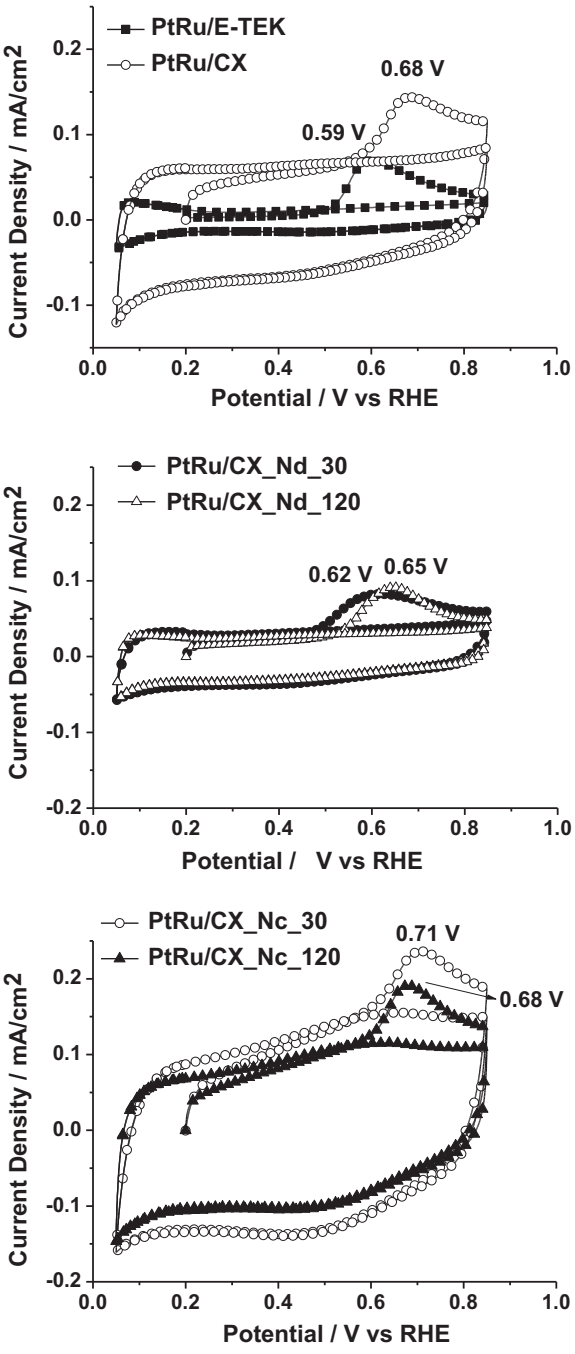

Fig. 11. Cyclic voltammograms during CO stripping in a 0.5 M H_2SO_4 solution at PtRu/CX catalysts and PtRu/E-TEK. Scan rate $\nu = 0.02\ V\ s^{-1}$.

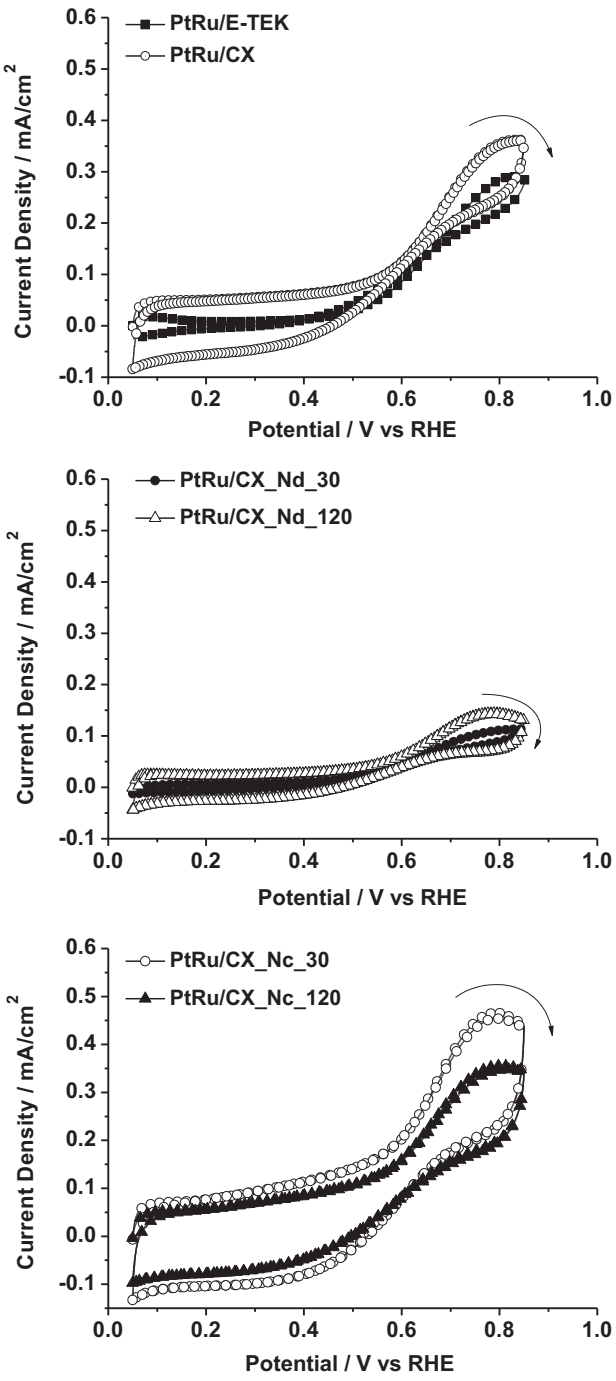

Fig. 12. Cyclic voltammograms for the electrooxidation of methanol in a 2 M CH_3OH + 0.5 M H_2SO_4 solution at PtRu/CX catalysts and PtRu/E-TEK. Scan rate $\nu = 0.02\ V\ s^{-1}$.

through the surface oxygen groups, may be responsible for the attributed higher activity of these materials for methanol oxidation [37,38,43].

These results were corroborated by the current density–time plots (Fig. 10) obtained in the same solution at 0.60 V (this value is selected considering that is near the working potential at DMFCs). The lowest current density was observed for the E-TEK material (approx. 45 $\mu A\ cm^{-2}$). For those catalysts prepared on the supports functionalized with concentrated nitric acid, the curves were not stable and a continuous decay with the time was registered. In fact, the highest current density values of all materials for $t < 350$ s were obtained with Pt/CX_Nc_30, but for $t > 350$ s, other materials presented better results. On the other hand, similar and stable current densities of around 60 $\mu A\ cm^{-2}$ (38% higher than E-TEK) were recorded for the catalyst prepared with the untreated or treated with diluted nitric acid xerogels.

3.3.2. PtRu catalysts supported onto functionalized xerogels

CO electrooxidation at PtRu/CX materials and PtRu/E-TEK are given in Fig. 11. It can be observed that, compared to Pt catalysts, the onset potential of the oxidation of CO was negatively shifted. This fact is explained by the presence of Ru, which helps to oxidize the CO_{ads} as it has been widely proven in literature [44,45]. For the commercial PtRu catalyst, the onset potential was established at 0.50 V and the oxidation peak at 0.60 V. For the prepared catalysts, the onset potential is very difficult to be determined

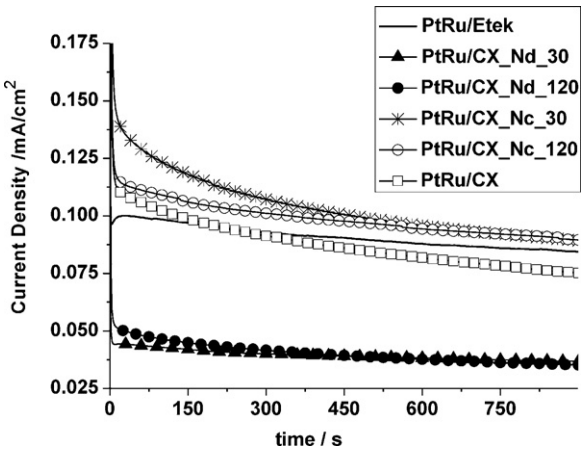

Fig. 13. Current density–time curves recorded in a 2 M H_2SO_4 + 0.5 M CH_3OH solution at E = 0.60 V vs. RHE for PtRu/CX catalysts and PtRu/E-TEK.

because of the double layer contribution presented by these materials (especially for those xerogels treated with concentrated nitric acid). However, the oxidation peak potential is clearly establish to be located positively shift with respect PtRu/E-TEK, the best results being obtained for the catalyst prepared with the supports functionalized with diluted nitric acid. According to these data, the more appropriate porous distribution of the xerogels with respect to the Vulcan as well as a high number of oxygen groups at the surface of the support, do not influence positively the oxidation of CO. It seems that only with an intermediate number of these oxygenated groups electrocatalytic properties of the catalysts are improved.

As in the case of Pt, the capacitive behaviour of the PtRu catalysts shows the trend of increasing for the CXs supported materials compared to the E-TEK and also with the strength of the oxidative treatment, being even more drastic than for Pt with a 10 times increment for PtRu/CX_Nc_120 and PtRu/CX_Nc_30.

The behaviour of the electrocatalysts towards the oxidation of methanol was studied in a deaerated 2 M CH_3OH + 0.5 M H_2SO_4 solution. Resulting voltammetric curves obtained are shown in Fig. 12. The onset potential of the methanol electrooxidation occurred at the same potential (around 0.50 V) for all PtRu catalysts.

Concerning the current densities at the peaks developed in the positive-going scan in the cyclic voltammograms, PtRu/CX_Nd_120 and PtRu/CX_Nd_30 presented the lowest values, whereas the best catalytic performance towards the oxidation of methanol were obtained with PtRu/CX_Nc_120 and PtRu/CX_Nc_30. Commercial PtRu/E-TEK and PtRu/CX show an intermediate behaviour. These results can be correlated with the amount of those oxygenated groups related with the production of CO_2 in Fig. 2 (carboxylic acids and lactones): the lowest amount of CO_2 is produced for CX treated with diluted nitric acid and the highest for the more drastic treatment, whereas untreated xerogel presents an intermediate production. Accordingly, it can be concluded that the carboxylic acids and lactones are involved in the increase of the catalytic activity towards methanol oxidation observed in the xerogels treated with concentrated nitric acid.

These results were corroborated by the current density-time plots (Fig. 13) obtained in the same solution at 0.60 V. The same sequence deduced from Fig. 12 can be established from the final values achieved after 15 min. It is noticeable that at the beginning of the curve, for time < 250 s, higher current values were observed with PtRu/CX_Nc_30, but current at this material was less stable with time than the curve for PtRu/CX_Nc-120).

4. Conclusions

Carbon xerogels were synthesized as support for Pt and PtRu catalysts. High mesoporous xerogels with suitable pore texture were obtained. Functionalization was carried out to create surface oxygen groups that favour the anchorage of metal particles on the support. The amount and the nature of surface oxygen groups created were determinant for the interaction carbon support-metallic particles, given that the more amount of surface oxygen groups, the more percentage of metal deposited.

CO stripping at Pt/CX catalysts showed that surface oxygen groups have some kind of participation in the oxidation of CO, lowering the potential at which CO begins to oxidize, compared to the commercial catalyst. This fact could be a benefit when used in PEMFCs.

Methanol oxidation at these Pt/CX catalysts begins at similar potentials than for the commercial catalyst, but still catalysts supported on carbon xerogels reach higher current density values, due to the presence of a higher amount of surface oxygen groups, improving the performance of the commercial catalyst, as corroborated by chronoamperometric curves.

All supports were used again for further preparation of PtRu/CX catalysts. Different results were obtained with these materials for CO electrooxidation: the stripping occurs at more positive potentials with the support which presents higher amounts of oxygen groups on the surface (but also higher metal content and higher crystallite size). In the case of methanol, the catalytic activity observed is related with the presence of carboxylic and lactone groups instead with the total amount of oxygenated groups.

In conclusion, functionalized xerogels with high surface areas, pore volumes and high content of surface oxygen groups, appear at a good alternative to carbon black supports for catalysts to be used in polymer electrolyte membrane and direct alcohol fuel cells.

Acknowledgments

The authors wish to thank “FEDER” and the Spanish MICINN for financial support (MAT2008-06631-C03-01 and MAT2008-06631-C03-02). OGV acknowledges Spanish MICINN. We also would like to give special thanks to F.J. Maldonado for all his kindly help. LC also acknowledges for her FPI grant.

References

[1] H. Liu, C. Song, L. Zhang, J. Zhang, H. Wang, D.P. Wilkinson, J. Power Sources 155 (2006) 95–110.
[2] A. Hamnett, Handbook of Fuel Cells—Fundamental, Technology and Applications. Volume 1: Fundamentals and Survey of Systems, 2003, pp. 305–322.
[3] C. Arbizzani, S. Beninati, E. Manferrari, F. Soavi, M. Mastragostino, J. Power Sources 172 (2007) 578–586.
[4] M.M.P. Janssen, J. Moolhuysen, Electrochim. Acta 21 (1976) 861–868.
[5] M. Watanabe, S. Motoo, J. Electroanal. Chem. 60 (1975) 275–283.
[6] J.B. Goodenough, A. Hamnett, B.J. Kennedy, R. Manoharan, S.A. Weeks, J. Electroanal. Chem. 240 (1988) 133–145.
[7] J. McBreen, S. Mukerjee, J. Electrochem. Soc. 142 (1995) 3399–3404.
[8] E. Miyazaki, Catalysis 65 (1980) 84–92.
[9] N. Tsiouvaras, M.V. Martínez-Huerta, R. Moliner, M.J. Lázaro, J.L. Rodríguez, E. Pastor, M.A. Peña, J.L.G. Fierro, J. Power Sources 186 (2009) 299–304.
[10] T. Frelink, W. Visscher, J.A.R. van Veen, Surface Science 335 (1995) 353–360.
[11] Z. Cui, C. Liu, J. Liao, W. Xing., Electrochim. Acta 53 (2008) 7807–7811.
[12] W.J. Zhou, W.Z. Li, S.Q. Song, Z.H. Zhou, L.H. Jiang, G.Q. Sun, Q. Xin, K. Poulianitis, S. Kontou, P. Tsiakaras, J. Power Sources 131 (2004) 217–223.
[13] J.L. Figueiredo, M.F.R. Pereira, P. Serp, P. Kalck, P.V. Samant, J.B. Fernandes, Carbon 44 (2006) 2516–2522.
[14] X. Yu, S. Ye, J. Power Sources 172 (2007) 133–144.
[15] M. Kim, J.N. Park, H. Kim, S. Song, W.H. Lee, J. Power Sources 163 (2006) 93–97.
[16] S.C. Hall, V. Subramanian, G. Teeter, B. Rambabu, Solid State Ionics 175 (2004) 809–813.
[17] E. Antolini, L. Giorgi, F. Cardellini, E. Passalcqua, J. Solid State Electrochem. 5 (2001) 131–140.
[18] L. Calvillo, M. Gangeri, S. Perathoner, G. Centi, R. Moliner, M.J. Lázaro, J. Power Sources 192 (2009) 144–150.

[19] E.S. Steigerwalt, G.A. Deluga, D.E. Cliffel, C.M. Lukehart, J. Phys. Chem. B 105 (2001) 8097–8810.
[20] D. Sebastián, I. Suelves, M.J. Lázaro, R. Moliner, J. Power Sources 192 (2009) 51–56.
[21] L. Calvillo, M.J. Lázaro, E. García-Bordejé, R. Moliner, P.L. Cabot, I. Esparbé, E. Pastor, J.J. Quintana, J. Power Sources 169 (2007) 59–64.
[22] N. Job, M.F. Ribeiro, S. Lambert, A. Cabiac, G. Delahay, J.F. Colomer, J. Marien, J.L. Figueiredo, J.P. Pirard, J. Catal. 240 (2006) 160–171.
[23] P.V. Samant, J.B. Fernandes, C.M. Rangel, J.L. Figueiredo, Catal. Today 102–103 (2005) 173–176.
[24] H.J. Kim, W.I. Kim, T.J. Park, H.S. Park, Suh.F D.J., Carbon 46 (2008) 1393–1400.
[25] R.W. Pekala, J. Mater. Sci. 24 (1989) 3221–3227.
[26] C. Moreno-Castilla, F.J. Maldonado-Hódar, Carbon 43 (2005) 455–465.
[27] C. Lin, J.A. Ritter, Carbon 35 (1997) 1271–1278.
[28] S.A. Al_Muhtaseb, J.A. Ritter, Adv. Mater. 15 (2003) 101–114.
[29] J. Marie, S. Berthon-Fabry, P. Achard, M. Chatenet, A. Pradourat, E. Chainet, J. Non-Cryst. Solids 350 (2004) 88–96.
[30] E.J. Zanto, S.A. Al-Muhtaseb, J.A. Ritter, Ind. Eng. Chem. Res. 41 (2002) 3151–3162.
[31] M.L. Anderson, R.M. Stroud, D.R. Rolison, Nano Lett. 2 (2002) 235–240.
[32] W.S. Baker, J.W. Long, R.M. Stroud, D.R. Rolison, J. Non-Cryst. Solids 350 (2004) 80–87.
[33] N. Job, J. Marie, S. Lambert, S. Berthon-Fabry, P. Achard, Energy Convers. Manage. 49 (2008) 2461–2470.
[34] C. Prado-Burguete, A. Linares-Olano, F. Rodríguez-Reinoso, C. Salinas-Martínez de Lecea, J. Catal. 115 (1989) 98–106.
[35] J.L. Figueiredo, M.F.R. Pereira, M.M.A. Freitas, J.J.M. Órfão, Carbon 37 (1999) 1379–1389.
[36] M.A. Fraga, E. Jordao, M.J. Mendes, M.M.A. Freitas, J.L. Faria, J.L. Figueiredo, J. Catal. 209 (2002) 355–364.
[37] J.L. Gómez de la Fuente, M.V. Martínez-Huerta, S. Rojas, P. Hernández-Fernández, P. Terreros, J.L.G. Fierro, M.A. Peña, Appl. Catal. B 88 (2009) 505–514.
[38] J.L. Gómez de la Fuente, M.V. Martínez-Huerta, S. Rojas, P. Terreros, J.L.G. Fierro, M.A. Peña, Catal. Today 116 (2006) 422–432.
[39] J.R.C. Salgado, E. Antolini, E.R. Gonzalez, J. Phys. Chem. B 108 (2004) 17767–17774.
[40] J.H. Zhou, Z.J. Sui, J. Zhu, P. Li, D. Chen, Y.C. Dai, W.K. Yuan, Carbon 45 (2007) 785–796.
[41] N. Mahata, M.F.R. Pereira, F. Suárez-García, A. Martínez-Alonso, J.M.D. Tascón, J.L. Figueiredo, J. Colloid Interface Sci. 324 (2008) 150–155.
[42] A. Piotr, Bazuła, An-Hui Lu, Jörg-Joachim Nitz, Ferdi, Schüth, Micropor. Mesopor. Mater. 108 (2008) 266–275.
[43] P.V. Samant, C.M. Rangel, M.H. Romero, J.B. Fernandes, J.L. Figueiredo, J. Power Sources 151 (2005) 79–84.
[44] J.R.C. Salgado, F. Alcaide, G. Álvarez, L. Calvillo, M.J. Lázaro, E. Pastor, J. Power Sources 195 (2010) 4022–4029.
[45] A.S. Aricò, S. Srinivasan, V. Antonucci, Fuel Cells 1 (2001) 133–161.
[46] D. Pantea, H. Darmstadt, S. kaliaguine, L. Sümmchen, C. Roy, Carbon 39 (2001) 1147–1158.
[47] A. Celzard, J.F. Marêché, F. Payot, G. Furdin, Carbon 40 (2002) 2801–2815.
[48] D. Sebastián, I. Suelves, R. Moliner, M.J. Lázaro, Carbon 48 (2010) 4421–4431.